Accepted Manuscript

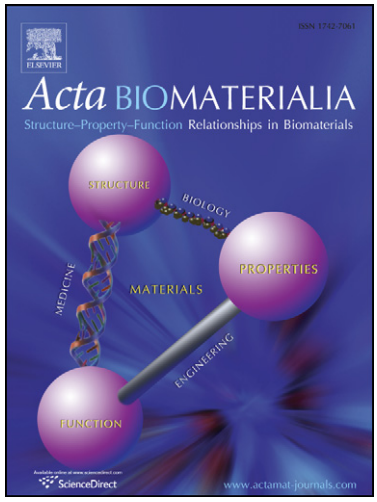

Development of remineralizing, antibacterial dental materials

Idris Mehdawi, Ensanya A. Abou Neel, Sabeel Valappil, Graham Palmer, Vehid Salih, Jonathan Pratten, Dave A. Spratt, Anne M. Young

PII: S1742-7061(09)00128-7
DOI: 10.1016/j.actbio.2009.03.030
Reference: ACTBIO 768

To appear in: *Acta Biomaterialia*

Received Date: 27 November 2008
Revised Date: 17 March 2009
Accepted Date: 24 March 2009

Please cite this article as: Mehdawi, I., Abou Neel, E.A., Valappil, S., Palmer, G., Salih, V., Pratten, J., Spratt, D.A., Young, A.M., Development of remineralizing, antibacterial dental materials, *Acta Biomaterialia* (2009), doi: 10.1016/j.actbio.2009.03.030

Development of remineralizing, antibacterial dental materials

Idris Mehdawi, Ensanya A. Abou Neel, Sabeel Valappil, Graham Palmer, Vehid Salih, Jonathan Pratten, Dave A. Spratt, Anne M. Young*

UCL Eastman Dental Institute, 256 Gray's Inn Road, London WC1X 8LD, UK

*Corresponding author.

Dr. Anne M. Young
Division of Biomaterials and Tissue Engineering,
UCL Eastman Dental Institute,
256 Gray's Inn Road,
London,
WC1X 8LD
Tel: +44 (0)20 7915 2353
E-mail address: A.Young@eastman.ucl.ac.uk

Keywords: Antibacterial, Reactive calcium phosphate, Raman, Biofilm, Chlorhexidine release, Compressive and biaxial flexure strength.

Abstract

Light curable methacrylate dental monomers containing reactive calcium phosphate filler [monocalcium phosphate monohydrate (MCPM with particle diameter 29 or 90 μm) and β-tricalcium phosphate (β-TCP) at 1:1 weight ratio] in powder : liquid ratio (PLR) 1:1 or 3:1 and Chlorhexidine Diacetate (0 or 5 wt%), were investigated. Upon light exposure, approximately 90 % monomer conversion was gained irrespective of the formulation. Increasing PLR promoted water sorption by the set material, induced expansion and enhanced calcium, phosphate, and chlorhexidine release. Concomitantly, a decline in compressive and biaxial flexural strengths occurred. With a reduction in MCPM particle diameter, however, calcium and phosphate release was reduced and less deterioration in strength observed. After 24 hours, remaining MCPM had reacted with water and β-TCP forming, within the set materials, brushite of lower solubility. This provided a novel means to control water sorption, component release and strength properties. Measurable chlorhexidine release was observed for 6 weeks. Both diffusion rate and total percentage of chlorhexidine release decreased with lowering the PLR or adding buffer to the storage solutions. Higher chlorhexidine release was associated with reduced bacterial growth on agar plates and in a biofilm fermenter. In cell growth media, brushite and hydroxyapatite crystals precipitated on the composite material surfaces. Cells spread on both these crystals and the exposed polymer composite surfaces indicating their cell compatibility. These formulations could be suitable antibacterial, biocompatible and remineralizing dental adhesives/liners.

1. Introduction

Dental composite materials, based on methacrylate monomers loaded with high levels of inorganic fillers, have been widely accepted for restoring either anterior or posterior teeth mainly for esthetic reasons. These materials depend on adhesive systems of largely similar chemical composition, but with lower filler content, as a means of bonding to tooth structures. A major drawback with dental composites, however, is polymerization shrinkage. This affects bonding integrity and can lead to gaps at the adhesive/tooth interface. These gaps increase the possibility for bacterial microleakage and secondary caries, which are the main causes of restoration failure [1].

Furthermore, a commonly used approach in modern management of carious lesions relies on removal of only outer infected dentine whilst inner reminerizable dentine is conserved [2]. The presence of residual bacteria within this dentine further increases the risk of reinfection and secondary caries. This is of particular concern when using dental composites as they lack any antibacterial properties. For this reason, bacteria tend to accumulate more below dental composites than other restorative materials such as amalgam [3].

There have been various attempts to develop antibacterial dental composites but significant problems such as reduction in mechanical properties and limited antibacterial action have arisen [4-7]. Since antibacterial properties are, however, primarily required at the dentine/restoration interfacial region, it should be more effective to include antibacterial agents within a restoration liner/base material or methacrylate adhesive. With these applications, material strength requirements are less stringent.

Conventional and resin modified glass ionomer cements have been applied as liner/base materials to improve marginal adaptation of composite restorations and reduce bacterial microleakage at the restoration/tooth interface [8]. Although these materials release fluoride, their anticariogenic effects have been attributed to their interaction with tooth hydroxyapatite and formation of a less soluble fluoroapatite rather than direct antibacterial action [9, 10]. Calcium hydroxide liners do have some antibacterial action. This is generally associated with their high pH, but these

materials generally also dissolve in tissue fluids or lack adhesion to dentin and other restorative materials [11-13].

Some dental adhesives may also exhibit antibacterial activity due to incorporation of acidic monomers [14]. This activity can be significantly reduced, however, after light curing or buffering by dentinal fluid [15, 16]. Gluteraldehyde incorporated within dental adhesives can also provide strong antibacterial action [17], but its volatility makes toxicity of significant concern [18]. Furthermore, although 1, 2-methacryloyloxydodecylpyridinium bromide (MDPB) is an effective antibacterial agent, it is bound in the set dental adhesive limiting its effectiveness to those bacteria in direct surface contact [19, 20]. We anticipate that a non bonded antibacterial agent that could be released and trapped under a restorative material would be more beneficial.

To gain good interlock between a composite and tooth structure, with a majority of adhesive methods currently employed, exposed dentine is first treated with 35% phosphoric acid gel. This leaves a layer of de - mineralized collagen within which fluid hydrophilic resin adhesives can penetrate and set but unfortunately with varying degrees of bonding and sealing effectiveness. In addition to antibacterial action, it would be beneficial therefore for dental liner/bases and adhesives to release calcium phosphate species. Early release could help re - mineralize and stabilize remaining defective tooth structure in addition to any acid - treated collagen which the adhesive resin fails to penetrate. Furthermore, longer term release might aid the repair of the adhesive / collagen hybrid layer that may become damaged by enzymatic action or thermal cycling and occlusal loading [21].

Recently, methacrylate resins containing various calcium phosphates as a filler phase have been formulated [21,22]. The use of combined reactive calcium phosphate fillers, β-tricalcium phosphate (β-TCP) and monocalcium phosphate monohydrate (MCPM) as in this investigation, however, has not previously been reported. When combined with water, these two compounds react via hydrogen ion exchange and re-precipitate as brushite (dicalcium phosphate dihydrate, $CaHPO_4.2H_2O$) or the anhydrous form, monetite [23].

Ideally, dental adhesives should be non toxic to pulpal tissues. When conventional adhesives are placed directly on or in close proximity to the pulp, however, they can induce severe pulpal inflammation [24]. This effect could in turn, enhance pulpal response to bacterial microleakage. Calcium phosphate based biomaterials are known to be highly cell compatible [25]. Cytotoxic effects with methacrylates occur mainly because of incomplete polymerization and release of unreacted free monomers [26]. One aim of this investigation is to assess whether cell compatibility of dental methacrylates could be affected via addition of reactive calcium phosphate fillers.

In this study chlorhexidine diacetate has been added into light curable dental methacrylate monomers that contain reactive calcium phosphate filler particles [β-TCP and MCPM]. Chlorhexidine diacetate, a broad spectrum antibacterial agent, has been used to disinfect excavated tooth cavities prior to restoration. In an attempt to increase the length of time over which this drug might be effective, however, it has additionally previously been incorporated into methacrylate based, filled [7] and unfilled resins [27]. It was, however, readily released only if significant water sorption occurred or drug loading was excessively high. In such situations, mechanical properties are likely to be very low and / or decline substantially with time.

Our hypothesis was that the addition of water-soluble MCPM fillers should encourage water sorption into the set resin materials, which in turn will enhance release of chlorhexidine and some calcium phosphate species. Subsequently, however, the absorbed water should promote reaction between MCPM and β-TCP and brushite formation within the polymerized methacrylate. As this reaction can bind water and encourage re - precipitation of less soluble species in material regions from which components have been released it was also anticipated that it might limit the reduction in strength normally associated with water sorption and component release.

Ultimately, the aim of this study was to formulate antibacterial and calcium phosphate releasing materials with appropriate mechanical and biological properties for potential use as a dental liner/base or adhesive underneath composite restorations. The following describes mechanical, microbiology and cell biology investigations on

systematically varying formulations. Chemical studies have also been performed to evaluate the degree of monomer conversion and in situ reaction of reactive calcium phosphate fillers.

2. Materials and methods

2.1. Materials and variables

Photo-activated resin was prepared by combining commercially available monomers, 2-hydroxyethyl methacrylate (HEMA) (Sigma-Aldrich), triethylene glycol dimethacrylate (TEGDMA) (Sigma-Aldrich) and urethane dimethacrylate (UDMA) (Rhom) in a fixed ratio 2:1:1 by weight, with 1 wt % camphorquinone (CQ) (Sigma-Aldrich) and 1 wt % dimethyl-p-toluidine (DMPT) (Sigma-Aldrich). The filler contained equal masses of MCPM (Sigma-Aldrich) and β-TCP (Fluka). β-TCP with particle diameter < 15 μm was used as received. The MCPM particles, however, were ground using a ball mill and passed through Endecotts sieves to obtain particles in the range: small (20-38 μm) with median diameter 29 μm and large (75-105 μm) with median diameter 90 μm. All formulations had high or low powder (filler) / liquid (resin) mass ratio (PLR) of 3:1 or 1:1 respectively. Chlorhexidine diacetate (CHX) (Sigma-Aldrich) was also incorporated at a level of 0 (i.e absent) or 5 wt % of the liquid phase.

Specimen storage solutions were either deionised water or phosphate buffer solution. The later was prepared by dissolving phosphate buffer saline tablets (Sigma-Aldrich) in 200 ml of deionised water. These gave solutions with 0.01 M phosphate buffer, 0.0027 M potassium chloride and 0.137 M sodium chloride and pH 7.4 at 25 ºC.

2.2. Sample preparation

The filler and monomers were mixed using hand spatulation for 30 seconds and the material poured into suitable steel moulds to produce discs of different forms. Circular discs of 10 mm diameter, 2 mm thickness and cylindrical discs of 4 mm diameter, 6 mm height was prepared for biaxial flexure (BFS) and compressive

strength (CS) measurements respectively. The fractured discs from BFS tests were subsequently used in Raman studies. Circular discs of 10 mm diameter, 1 mm thickness were prepared for water sorption, CHX and ion release, agar diffusion and biocompatibility investigations. For bacterial biofilm studies, discs of 5 mm diameter and 1 mm thickness were prepared. Photopolymerization of all samples was initiated by irradiation top and bottom for 60 seconds with a blue light-curing unit (L.E. Demetron I, Kerr, USA), for which the power output was 1000 mW/cm^2.

2.3. Degree of monomer conversion and brushite formation

Raman microscopy was used to quantify the level of monomer conversion and changes in filler chemistry upon light exposure and subsequent water sorption respectively. To aid peak assignment, spectra were generated of all the pure components, brushite and the polymerized monomer. All possible combinations of high and low PLR and MCPM particle diameter, in addition to CHX concentration [giving 8 possible formulations, Table 1 (a)] were examined.

Surface Raman spectra were obtained before light cure and at 24 h post irradiation with and without an additional subsequent immersion in deionised water for various periods up to 24 h. Variations in chemistry with depth were additionally assessed by analysis of fracture surfaces of BFS specimens. All spectra were obtained using a Lab Ram spectrometer (Horiba, Jobin Yvon, France). The samples were excited at 633.8 nm by a He-Ne laser through a microscope objective (×50). Raman spectra were obtained in the region 800-1700 cm^{-1} with resolution 2 cm^{-1} using a confocal hole of 300 μm, giving an approximate spatial resolution of 5 μm. To gain representative average spectra several hundred point spectra for each sample were generated and averages gained. After baseline subtraction, these average spectra were normalized using a peak that was not significantly affected by polymerization (1455 cm^{-1}, C-H stretch bond). % degree of monomer conversion was then calculated using equation (1) [28,29]:

$$\%\ \text{degree of conversion} = \frac{100[A_0 - A_t]}{A_o} \qquad (1)$$

A_0 and A_t are the peak height of the C=C stretch peak at 1638 cm^{-1} before and after polymerization respectively.

Qualitative determination of water sorption induced brushite formation was assessed as a function of depth through relative changes in various phosphate peak heights around 1000 cm^{-1}. Raman P-O stretch peaks of β – TCP are at 943 / 968, MCPM at 901/912/1011 and brushite at 986 cm^{-1} [29,30]. These are well separated from typical major methacrylate peaks [29] or those of chlorhexidine (at 1286 / 1292 and 1597 cm^{-1}) [30] and therefore easy to identify.

2.4. Compressive and biaxial flexure strength

Compressive strength (CS) and biaxial flexure strength (BFS) of all possible formulations were determined before and after 24 h and 1 week of immersion in deionised water using a computer - controlled universal testing machine (Instron 4502, UK) using 8 specimens of each formulation. For BFS, the samples were placed on a knife-edge ring support of 8 mm diameter and the load applied using a 4 mm diameter spherical ball indenter at 1 mm/min crosshead speed. The failure stress was recorded and BFS calculated using equation (2):

$$BFS = \frac{\rho}{l^2}\left\{(1+\nu)\left[0.485\ln\left(\frac{a}{l}\right)+0.52\right]+0.48\right\} \qquad (2)$$

ρ is the load at failure, l is the sample thickness, a is the radius of knife-edge support and ν is Poisson's ratio (0.225) [31].

Compressive strength specimens were loaded at a crosshead speed of 1 mm / min and calculated using equation (3):

$$CS = \frac{\rho}{\pi r^2} \qquad (3)$$

r is the radius of the sample.

2.5. Mass and volume changes

The mass and volume of formulations containing CHX, PLR 1:1 or 3:1 and MCPM particle diameter 29 or 90 μm were measured gravimetrically using a four figure balance (Mettler Toledo) with attached density kit. Each specimen was placed upright in the conical end of a sterilin tube, allowing contact of both sides with 10 ml of either deionised water or phosphate buffer solution. The tubes were then incubated at 37 ºC for 1, 2, 3, 4, 6, 24, 48 h and 1, 2, 3, 4, 5, 6 weeks. At each time point, the specimens were removed, blotted dry, reweighed, and placed in new tubes containing fresh storage solution. The percentage volume and mass change at each time was finally determined from equation (4) and (5) respectively:

$$\%\ \text{Volume change} = \frac{100[V_t - V_o]}{V_o} \tag{4}$$

$$\%\ \text{Mass change} = \frac{100[M_t - M_o]}{M_o} \tag{5}$$

V_t and M_t are the volume and mass at time t after immersion, while V_o and M_o are the initial volume and mass respectively. Each formulation was examined in triplicate.

2.6. Chlorhexidine release

Absorbance of the above storage solutions between 200 and 400 nm were recorded using a UV spectrometer (Unicam UV 500, Thermospectronic®) and checked to ensure they had the same profile as spectra of pure CHX solutions. The amount of CHX released (R in grams) was then calculated using equation (6):

$$R = \frac{A}{g}V \tag{6}$$

A is the absorbance at 255 nm, g is the gradient of a calibration curve of absorbance versus CHX concentration (obtained using known solutions [30]) and V is the storage solution volume. The % cumulative amount of drug release ($\%R_c$) at time t was then given by equation (7):

$$\%R_c = \frac{100\left[\sum_0^t R_t\right]}{w_c} \quad (7)$$

w_c is the weight of CHX incorporated in the formulation in grams.

2.7. Calcium and phosphate ion release

Three different formulations containing CHX with PLR of 1:1 or 3:1 and MCPM particle diameter 29 μm or PLR of 1:1 with MCPM particle diameter of 90 μm were prepared in triplicate. All specimens were subsequently stored at 37 °C in 10 ml deionised water. Storage solutions were replaced with fresh deionised water at 1, 2, 3, 4, 6, 24, 48 h, 1, and 2 weeks. Calcium (Ca^{2+}) and phosphate (PO_4^{3-}) concentrations in storage solutions were determined using ion chromatography (Dionex, UK) and calibration solutions of calcium chloride or sodium phosphate standards of various ppm concentrations. Results were converted from ppm to mM and the cumulative release for Ca^{2+} and PO_4^{3-} calculated using equation (8) and (9) respectively:

$$I_{mM} = \frac{I_{ppm}}{M_w} \quad (8)$$

$$C_I = \sum_0^t [I_{mM}]_t \quad (9)$$

Where I_{mM} and I_{ppm} is ion release in mM and ppm respectively, while M_w is the molecular weight of Ca^{2+} or PO_4^{3-} and C_I is the cumulative ion release.

2.8. Antibacterial studies

In antibacterial studies, in addition to CHX-containing experimental samples, one formulation with PLR 3:1 but no CHX and the commercial resin modified glass ionomer cement (RMGIC), Fuji II LC improved (GC corporation) were used as controls.

2.8.1 Agar diffusion assay

In agar diffusion assays (BASAC Disk Diffusion Method for Antimicrobial Susceptibility Testing, Version 1, 2007), isosensitest agar (Oxoid) plates were inoculated with standardized cultures of *Streptococcus mutans* (NCTC 10449), *Lactobacillus casei* (NCTC 6375) or *Actinomyces naeslundii* (NCTC 10951). Three discs of each formulation with PLR 1:1 or 3:1 and MCPM particle diameter of 29 μm or PLR 1:1 with MCPM particle diameter 90 μm were prepared and then placed aseptically onto inoculated plates. All plates were incubated at 37 °C in a 5 % CO_2 atmosphere for 48 h except for those containing *Actinomyces naeslundii* that were incubated anaerobically for 72 h. The inhibition zones were measured at three different points using callipers.

2.8.2 Biofilm study

A CDFF (Constant Depth Film Fermentor; University College Cardiff, UK) described previously [32] was used to grow oral microcosm biofilms at 37°C. Formulations with PLR of either 1:1 or 3:1 and MCPM particle diameter 29 μm were evaluated. Nine discs of each formulation were placed on plugs recessed in 5 mm diameter PTFE pans, which were then inserted flush with a stainless steel turntable beneath fixed PTFE scrapper blades. The samples themselves were recessed 300 μm below these blades to provide space for biofilm growth.

Saliva was collected from 10 healthy individuals, and an equal amount from each mixed with 10 % glycerol (v/v) and stored at -70°C. As required, one cryovial containing 1 ml pooled saliva was defrosted and used to inoculate 500 ml of sterile artificial saliva [33]. This was passed through the CDFF at a flow rate 0.5 ml/min (approximate salivary flow rate in humans) for 8 h followed by sterile artificial saliva at the same rate for the remainder of the experiment. The turntable speed was fixed at 3 rpm.

Three discs of each formulation were removed aseptically from the CDFF after 6, 24 and 72 h and vortexed for 1 min in 1 ml of phosphate buffer saline (Oxoid). Following serial dilution, 25 μl of this phosphate buffer solution was plated onto fastidious anaerobic agar plates (Oxoid). The agar plates were incubated

anaerobically at 37 °C for 5 days and then the number of colony-forming units (CFU) determined.

2.9. Biological assessment

An *in vitro* attachment study of human osteoblast-like cells (MG63, an osteosarcoma line) was performed to assess the biocompatibility of formulations with PLR 1:1 or 3:1 with 0% CHX and small MCPM particle diameter. Results were compared with unfilled copolymer and Thermanox® (surface treated polyethylene terephthalate) as control surfaces. Prior to culture, all samples were sterilised by UV exposure for 30 min each side, and pre-treated by incubation for 24 h in culture medium [Dulbecco's modified Eagles Medium (DMEM, Gibco)] supplemented with 10 % (v/v) foetal calf serum and 1 % (v/v) penicillin and streptomycin solution (Gibco). The cells were then seeded at a density of 2.5 x 10^4 cells / disc in 6-well culture plates. After 24 h, the samples were fixed overnight with 3 % glutraldehyde in 0.1 M sodium cacodylate buffer (Agar Scientific Ltd., Essex, UK) at 4 ºC and then dehydrated in a graded series of alcohols (20, 50, 70, 90, and 100 %). The dehydrated samples were critically dried in hexamethyldisilazane (HMDS, Taab Laboratories Ltd., Berkshire, UK) for 1 min, and then left to air dry in a desiccator. The processed samples were finally mounted on aluminium stubs, sputter coated with gold-palladium alloy (Polaron E5000), and viewed using a scanning electron microscope (SEM: Cambridge 90B, Leica, UK) supplied with energy dispersive X-ray microanalysis (EDX: Inca 300, Oxford Instruments Analytical, UK).

2.10. Theory and statistical analysis

The early stages of diffusion controlled properties such as water sorption and drug release for flat discs can often be given by equation (10) [34]:

$$\Delta M = 100 M_\infty \sqrt{\frac{2Dt}{\pi l^2}} \qquad (10)$$

2l, D and t are the sample thickness, a diffusion coefficient and time respectively. ΔM represents the change in mass, volume or cumulative drug in solution. M_∞ is the maximum change. In the following, all these properties are plotted as a function of

the square root of time to enable clear visualisation of trends at both early and late time points. Initial gradients of these plots and maximum or final values were determined and analysed using the factorial analysis expressions given below.

A suitable factorial expression to analyse kinetic or equilibrium data from 8 samples with 3 variables each with 2 possible values would be [35, 36]

$$\ln P = <\ln P> + F_1 a_1 + F_2 a_2 + F_3 a_3 + F_1 F_2 a_{1,2} + F_1 F_3 a_{1,3} + F_2 F_3 a_{2,3} + F_1 F_2 F_3 a_{1,2,3} \quad (11)$$

F can have values of +1 or -1 only. In the following, F_1 and F_2 equal +1 or -1 when the PLR and MCPM particle diameter is high or low respectively. F_3 is +1 or -1 when CHX concentration is high or low or the storage solution water or buffer respectively. <lnP> is the arithmetic mean of 'ln P' for all 8 possible formulations.

$2a_i$ quantifies the average effect of changing variable 'i' and was calculated using:

$$2a_i = <\ln P>_{F=+1} - <\ln P>_{F=-1} \quad (12)$$

$<\ln P>_{F=+1}$ and $<\ln P>_{F=-1}$ are the arithmetic mean values of ln P for all four samples with F_i equal to +1 and -1 respectively. $a_{i,j}$ and $a_{i,j,k}$ are two and three variable interaction terms. These were calculated using:

$$2a_{ij} = <\ln P>_{FiFj=+1} - <\ln P>_{FiFj=-1} \quad (13)$$

$$2a_{ijk} = <\ln P>_{FiFjFk=+1} - <\ln P>_{FiFjFk=-1} \quad (14)$$

95 % confidence interval error bars for 2a parameters were calculated assuming C.I = 1.96 × S.D/√n. If these error bars cross zero, the variable 'i' has no significant effect on the property.

It should also be noted that the exponent of <lnP> equals the geometric mean of P. From equation 12 the exponent of $2a_i$ is also the ratio of the geometric mean result for all samples with F_i=+1 divided by that when F_i=-1. In other words, it is the factor by which a property on average alters when one variable is changed.

Data from mechanical tests were also analysed using the above factorial methods. Ion release and antibacterial results were analysed using independent-student-t test assuming normal distribution of the data and equality of variance at a significance level of < 0.05.

3. Results

3.1. Degree of monomer conversion and brushite formation

Due to composite specimen inhomogeneity and micron scale spatial resolution of the Raman microscope, point spectra of dry samples tended to be dominated by either a mixture of polymer / monomer / CHX peaks (i.e the drug filled matrix phase) or were identical to the spectrum of either β- TCP or MCPM. After water immersion point spectra had a mixture of organic and inorganic peaks.

Fig. 1 shows example average Raman spectra for one specimen before polymerisation, at 24 hours post cure and after subsequent submersion in deionised water for 24 h. At 24 h post cure, the vinyl C=C stretch peak at 1638 cm^{-1}, relative to the saturated C-H stretch peak at 1455 cm^{-1}, decreased substantially in all spectra. The average degree of conversion was approximately 90 % (Table 1.a) and not significantly affected by any variable (see small $2a_i$ values in Fig. 2). A comparable level of conversion was also observed with the unfilled polymer (data not shown).

Relative heights of different phosphate peaks could vary substantially with region selected for examination with the Raman microscope. Additionally, high fluorescence by some phosphate particles could prevent low noise Raman spectra being generated in some areas. Only qualitative interpretation of the phosphate peaks was therefore attempted.

Before submersion in deionised water, phosphate peaks (P-O stretch) at 901, 912 and 1188 cm^{-1} due to MCPM, and at 943 and 968 cm^{-1} for β- TCP were clearly observed in averaged Raman spectra of both unpolymerized and polymerised specimens. After 24 h immersion in deionised water, however, the peaks attributed to β - TCP and MCPM were substantially reduced in intensity relative to the polymer C-H peak at 1455 cm^{-1}. In their place a brushite peak at 986 cm^{-1} (P-O stretch) became visible. Irrespective of formulation, brushite was formed throughout the sample thickness, although low levels of unreacted β-TCP also remained in some regions of some samples (see for example Fig. 1).

3.2. Compressive and biaxial flexure strength

Geometric average CS and BFS for all formulations decreased from 87 and 61 down to 32 and 27 MPa upon 24 h storage in water (Table 1a). Conversely, the initial CS and BFS for unfilled polymer were 140 and 88 MPa respectively, and little changed after 24 h immersion in water. As all $2a_i$ values are comparable with or smaller than 95 % CI error bars (Fig. 2) none of the studied variables had a significant effect on the dry composite strength. With smaller MCPM particle diameter, however, the decline in strength in water was reduced (note negative $2a_i$ value in Fig. 2 for MCPM diameter). The average wet CS and BFS, increased from 27 and 22 to 38 and 32 MPa respectively upon lowering MCPM particle diameter by three fold. Between 24 hours and 1 week of water immersion, no significant change in either CS or BFS was observed (see Table 1a).

3.3. Mass and volume changes

Composite mass and volume change were both proportional to the square root (SQRT) of time for the first 6 h (see for example Fig. 3) as expected from equation 10. After 24 hours these properties slowly declined as water sorption reached equilibrium and further changes due to material loss exceeded the effects of any further water sorption gain. The geometric average initial gradient of mass change was 0.17 wt %/$min^{0.5}$. The average results at high and low PLR were 0.26 and 0.12 wt % /$min^{0.5}$ respectively (Table1.b). Factorial analysis showed raising PLR increased this gradient most. It also revealed that increasing PLR caused the greatest increase in the maximum mass and volume. Removal of buffer from the storage solution had a smaller effect and MCPM particle diameter and variable interactions no significant effect on these properties (Fig. 4).

For all formulations, the volume change was generally double that of mass change. Geometric average volume and mass change for all formulations reached a maximum of 19 % and 9 % at 24 hours respectively (Table 1. b). They then slowly declined over the following 6 weeks to final values of 13 % and 7 % respectively. Factorial analysis (Fig. 4) suggests that factors affecting maximum mass change had within experimental error the same effect on maximum volume change.

3.4. Chlorhexidine release

The level of CHX release was proportional to the square root of time for a longer period than mass and volume changes as evidenced from Fig. 3 and 5. After 4 weeks (square root time, t=200 $min^{0.5}$ in Fig 5), release rates had substantially declined despite total CHX release being significantly below 100 %. Geometric mean of the initial gradient of CHX release, drug diffusion coefficient and total CHX release for all formulations were 0.38 wt %/$min^{0.5}$, 0.09×10^{-8} cm^2/s and 53 wt% respectively as given in Table 1 (b). Factorial analysis (Fig. 4) indicated that increasing the PLR caused the greatest increase in both the early release rate and later time total CHX release. Upon increasing the PLR from 1:1 to 3:1, the gradient of CHX release and diffusion coefficient increased on average by a factor of 2 and 3.8 respectively, whereas the total release increased by a factor of 1.6. Removal of buffer increased the gradient of CHX release and diffusion coefficient by a factor of 1.4 and 2 respectively, whereas the total release increased by a factor of 1.3. The effects of MCPM particle diameter and variable interactions were negligible.

3.5. Calcium and phosphate release

The cumulative Ca^{2+} and PO_4^{3-} release from all samples exhibited a burst release for the first 24 hr after which the release continued at a much slower rate (see for example Fig. 6). Early release of PO_4^{3-} was greater than that of Ca^{2+} but after 24 hours, release rates for the two ions were comparable. By comparing the total Ca^{2+} and PO_4^{3-} release after 2 weeks (Fig. 7), the formulations with high PLR released significantly more Ca^{2+} and PO_4^{3-} than low PLR ($P < 0.05$). Moreover, the formulations with large MCPM particle diameter exhibited significantly more $Ca^{2+}$and PO_4^{3-} release than formulations with small MCPM particle diameter ($p < 0.05$).

3.6. Antibacterial Studies

All CHX containing test materials gave inhibition zones in agar diffusion tests (Fig. 8) in contrast to the control samples that gave no observable antibacterial activity. For all tested bacterial species, the size of inhibition zones significantly increased upon raising PLR from 1:1 to 3:1 ($P<0.05$) while varying MCPM particle diameter showed

no significant effect (P>0.05). The effect of PLR was particularly pronounced with *A. naeslundii*.

From the biofilm study (Fig. 9), the CHX-containing formulations (II and III) showed the most inhibition of growth at all time points compared to the control samples (Formulation I and Fuji II LC) ($p < 0.05$). At 6 hr and 72 hr, Formulation III (with 3:1 PLR) inhibited growth slightly better ($P < 0.05$) than Formulation II (with 1:1 PLR).

3.7. Biological assessment

After 24 hr in cell culture medium crystals with calcium / phosphorus ratios of either 1.0 or 1.67 (EDX analysis) could be detected precipitated on the surfaces of experimental formulations containing filler (see Fig. 10c and d). The formulation with 3:1 PLR seemingly had more area covered by crystals than that with PLR 1:1. These crystals were not observed on unfilled copolymer, thermanox® or dry composite samples. MG63 cells showed attachment and migration on both the experimental formulations containing filler as well as to unfilled copolymer (Fig. 10b) and thermanox® (see Fig. 10a). The cytoplasmic extensions from the cells spread over the composite surface and towards crystals of variable shape and size.

4. Discussion

Bioactive and antibacterial methacrylate resins incorporating both reactive calcium phosphate fillers and chlorhexidine have been developed for potential application as dental liner/base or adhesive materials. The antibacterial activity of this system has been assessed using both a simple agar diffusion method and a more sophisticated biofilm study. The remineralising potential was initially monitored by considering the level of calcium and phosphate release. Moreover, the effect of such inclusion on the polymer properties was also considered from the chemistry, mechanical, and biocompatibility point of view.

4.1. Degree of monomer conversion and brushite formation

The resin monomers in adhesive formulations of this study showed a high level of polymerization (~ 90 %) upon photo-initiation. Generally, methacrylates in dental composites have lower polymerization levels (between 39 and 79 %) [28]. The high degree of polymerization obtained in this study could be attributed to incorporation of high content of HEMA (50 wt %) which is often added to dental adhesives to raise their hydrophilicity and hence their wetting ability to dentin [37]. The reduced monomer viscosity and raised polymer flexibility upon HEMA addition, decreases the glass transition temperature (T_g) of the resin matrix and increases the mobility of reactive species thereby enhancing degree of conversion [38]. High monomer conversion can improve the biocompatibility, as unreacted monomers are then less likely to penetrate into pulpal tissues and cause an inflammatory reaction. Good biocompatibility is important if the material is to be used as dental liner or composite adhesive, particularly when remaining dentin thickness is minimal. Disadvantages of high polymerization, however, include greater heat generation and polymerization shrinkage both of which are proportional to the degree of conversion [39, 40].

Generally, addition of filler particles could potentially reduce the rate of methacrylate polymerization particularly if there is mismatch in filler / resin refractive indices and significant specimen opacity. Higher filler level or small particles can additionally, if particles are poorly wet by the monomer, inhibit the polymerization by increasing the chance of air bubble incorporation [41]. On the other hand, CHX addition can increase methacrylate polymerization rate [7]. In this study, however, at 24 hours, increasing both particle diameter and filler mass fraction or adding CHX had no significant effect on vinyl conversion level.

MCPM particles were included in the above samples to encourage water sorption and thereby enhance CHX, calcium and phosphate release. With MCPM alone, these processes are too extensive leading to excessive material degradation. Additionally, with no filler or only β-TCP in the methacrylate monomers of the above study, the CHX release was highly restricted (data not shown). Incorporation of both highly degradable MCPM and relatively insoluble β-TCP as a reactive filler was attempted to provide a control on water sorption, and ion release. Through MCPM reaction with water and β-TCP, lower solubility brushite, can form within these

composites providing a novel means to control water sorption and component release processes. Raman can be used to distinguish various different calcium phosphate species [29, 30, 42]. In this investigation, Raman mapping studies proved that brushite formation occurred throughout the sample thickness within 6 hr of water immersion irrespective of the formulation.

As the molecular weight of β-TCP (310g/mol) is slightly greater than that of MCPM (252 g/mol), with equal weights of the two, the latter is in excess in the above formulations by 19 wt%. MCPM, however, is more water soluble than β-TCP and therefore more likely to be released from the materials at early times. If more that 19 wt% of the MCPM is released then β-TCP will be in excess and should be (and is in some cases) observed in Raman spectra after 24 h submersion in water.

4.2. Compressive and biaxial flexure strength

The dry composite materials had significantly lower mechanical properties than the unfilled resin. A likely cause is lack of interaction between the filler and resin matrix making the organic / inorganic interface a point of weakness. All the studied formulations additionally exhibited a much greater decline in compressive and biaxial flexure strength after 24 hr of immersion in deionised water than the unfilled copolymer. This is presumably due to the soluble MCPM encouraging high water sorption, which is considered a key factor reducing composite mechanical properties. This occurs via plasticization and disruption of the polymer matrix [43]. Filler release arising upon water sorption will also, however, be a contributory factor causing decline in strength. The lack of further deterioration in strength between 24 hr and one week of water immersion is likely due to both cessation of water sorption and substantial reduction in calcium phosphate release rate during this period.

The addition of CHX in these new formulations did not affect the mechanical properties. This is in contrast with an earlier report, which demonstrated a substantial decline in both tensile and compressive strengths of dental composites with addition of 5% of chlorhexidine [44]. This discrepancy could be attributed to the form of CHX salt used; acetate (in this study) versus gluconate (in the former study).

Increasing PLR from 1:1 to 3:1 had no effect on either compressive or biaxial flexure strength of either dry or wet samples. Formulations with small MCPM particle

diameter, however, exhibited a lesser reduction in mechanical strength in water. This is likely due to a reduced percentage of calcium phosphate release from the specimens (see below).

The above new formulations showed a greater decline in strength in water than similar amorphous calcium phosphate (ACP) composites [45-47]. A likely major cause is higher percentage filler loss in this study arising from greater solubility of MCPM compared with ACP.

The compressive strength of all formulations in this investigation exceed those of conventional self curing calcium hydroxide (14-27 MPa) [48], and are comparable to polymer reinforced zinc oxide eugenol, a commonly used liner/base and temporary restorative material (38 MPa) [49]. Zinc oxide eugenol cements, however, could not be used with composite restorations due to their retardation effect on methacrylate polymerization. Consequently, our formulations could, without modification, be used as a liner/base and temporary restorative materials with added benefits of simultaneous Ca^{2+}, PO_4^{3-} and CHX release.

4.3. Volume and mass changes

The high initial increase in mass and volume of the composite samples is likely due to the presence of MCPM whose dissolution in absorbed water enhances osmotic pressure. As observed in a previous study with amorphous calcium phosphate composites, maximum water sorption was approximately proportional to the filler mass fraction [50,51]. In this study, raising PLR was also observed to cause an even greater effect on the initial rate of water sorption. According to the following equation, for every gram of MCPM, 0.5 g of water is required for formation of brushite [23].

$$Ca_3 (PO_4)_2 + Ca (H_2PO4)_2.H_2O + 7H_2O \rightarrow 4CaHPO_4.2H_2O$$

For full reaction of all the MCPM with PLR 3:1 and 1:1, 18.7 and 12.5 wt % water therefore needs to be absorbed. The average maximum mass increase (due to combined water sorption and MCPM loss) was 10.8 and 7.7 wt% for formulations

with PLR 3:1 and 1:1 respectively. From the percentages of MCPM lost (21 – 29 wt % see below) these figures suggest that slightly less water is absorbed than required for full reaction of all the MCPM remaining in the composites.

Formulations immersed in phosphate buffer exhibited less water sorption than those in deionised water. This could be explained by a reduced osmotic gradient between the aqueous droplets inside the polymer (containing dissolved calcium and phosphate species), and the external solutions. This could indicate that the high water sorption of the formulations in this study is an osmotically driven process. The reproducible decrease in the mass and volume of the samples over longer periods may be due to some limited slow filler loss but also water being forced out of the polymer matrix upon reduction of osmotic pressure when the fillers precipitate as brushite. The final mass and volumes were stable by the end of the experiment but always greater than initial values. This was due to the additional volume of the water, which was bound within brushite, exceeding the mass and volume of any components released.

4.4. CHX release

Early release of CHX from the materials was proportional to the square root of time as expected for a diffusion-controlled process, but at longer times the release substantially slows possibly because of binding of absorbed water in brushite crystal structures. CHX release will have limited effect on mass and volume changes because its percentage mass is relatively low and it is likely to be replaced in the bulk of the material by water of similar density.

Increasing MCPM and β-TCP filler mass fraction substantially enhanced the release of CHX. Release of this drug also continued for several weeks despite most of the water absorbed in the first 24 hours rapidly becoming bound in brushite crystal structures. A possible explanation is that precipitation of brushite gives a composite structure with channels through the polymer that allow drug diffusion.

The reduction in CHX release upon buffer addition to the storage water may be due to reduced water sorption of the samples (see results of mass changes).

Another explanation could be related to the cationic nature of CHX, which may bind to anions in the phosphate buffer solutions (phosphate and chloride) to form salts of lower solubility.

Compared with other CHX releasing resins, the experimental formulations in this study can give high percentage release that is between 27 and 70 wt% in two weeks. Composites produced using the same monomers as in this study but fluroroaluminosilicate glass filler, released only 5.4 % CHX over a similar time period [7]. This could be increased by raising water sorption via enrichment of HEMA content of the resin matrix, but this substantially decreases composite strength. In the above study, the addition of reactive calcium phosphate fillers rather than increasing HEMA content could be a more appropriate approach to encourage CHX release from matrix resins, particularly with the remineralization benefits of the calcium phosphate filler.

With unfilled UDMA/TEGDMA based resin, estimates suggest it would take several years to release 50% of entrapped CHX at pH = 6 [27]. Furthermore, a self curing system based on poly (ethylmethacrylate) and tetrahydrofurfuryl methacrylate exhibited a release of only 6-12 % of incorporated CHX over 14 days [52]. Fast early release of CHX is important to eliminate residual bacteria and/or early colonisation of the gaps between a tooth and restoration and this could be particularly useful if the drug can then be trapped within such gaps. Such entrapment might be improved for example by placement of a stronger composite material on top of the new material.

CHX is known to beneficially interfere with endogenous enzymatic degradation of collagen [53]. In addition, the release of CHX from the new adhesive formulations into acid etched / demineralised dentine could therefore also potentially improve bond durability. It is further anticipated that co-release with calcium phosphate could help binding and entrapment of CHX within the adhesive / collagen hybrid layer. Longer term CHX release from the material or additionally the hybrid layer could then help prevent bacterial microleakage within gaps that form upon bond failure due to occlusal loading and thermal cycling.

4.5. Calcium and phosphate release

The reactive filler in the above formulations enabled burst release of Ca^{2+} and PO_4^{3-} in the first 24 hr of sample immersion in deionised water but this was followed by a substantial decline in release rate for the remaining experimental period. The initial burst release could be explained by largely surface dissolution of the fillers particularly the MCPM which has higher solubility compared with β-TCP (K_{sp}= 7.18 × 10^{-2} and 2.07×10^{-33} at 25 °C, respectively) [54]. Some of this MCPM could, however, be from the core of the specimens if calcium phosphate diffusion through the polymer matrix is faster than reaction and brushite precipitation. The ratio of Ca^{2+} to PO_4^{3-} release was consistent with significantly more MCPM dissolution than β-TCP (molar ratio of Ca^{2+}/PO_4^{3-} is 0.5 and 1.5 in MCPM and β-TCP respectively). After 24 hr, the release of MCPM decreased presumably due to elimination of all MCPM from the material either by dissolution or brushite formation.

Brushite has low aqueous solubility compared to MCPM (K_{sp}= 2.59 ×10^{-7} at 25 °C) [54]. Any excess water in the materials could therefore, after brushite is formed be expelled from the material due to a lowering of osmotic pressure. Since calcium and phosphate release is low at later times, this could in part provide an alternative explanation for the slight reduction in material mass and volume after 24 hours.

Increasing filler mass fraction from 50 to 75 % enhanced the release of Ca^{2+} and PO_4^{3-} presumably because of increased water sorption as well as ion source. This effect was also observed in previous studies of Ca^{2+} and PO_4^{3-} release from calcium phosphate based resin composites [22].

Slightly increased ion release from formulations with larger MCPM particle diameter may be due to a higher concentration of this chemical being in direct contact with the sample surface. MCPM lower down in the sample is clearly able to largely react within the material before it can be released through diffusion. Bioactive composites based on ACP also exhibited reduced release of Ca^{2+} and PO_4^{3-} ions upon decreasing particle diameter [46], which was attributed to better interaction between the smaller filler particles and polymer matrix.

The level of Ca^{2+} and PO_4^{3-} release after 2 weeks is consistent with approximately 21wt % MCPM filler loss for formulations with small particle diameter

irrespective of PLR. With larger MCPM particle diameter the percentage loss is slightly higher at 26 wt%. There is therefore a slight excess of βTCP in the materials after water immersion, which would explain detection of low levels of this component in later time Raman spectra.

In summary, the above results suggest that the level of calcium and phosphate release is dependent upon the amount of MCPM in contact with the material surface. This could be increased either by raising the PLR, the ratio of MCPM to β TCP or the MCPM particle diameter. In previous studies of calcium phosphate bioactive composites, release of Ca^{2+} and PO_4^{3-} was proven to enhance mineral content of artificially demineralized human teeth [55]. Exactly how much calcium phosphate is required, however, is expected to be dependent upon the thickness of the demineralized layer.

It should be noted that vital pulpal tissues themselves have the ability to re - mineralize and repair carious tooth structures [56]. This regenerative capacity, however, can be reduced by bacteria enhanced inflammation [57,58]. Furthermore, additional calcium ions can stimulate differentiation of mineral forming cells in the pulpal tissues [59]. Materials that release both antibacterial and calcium containing components might therefore improve repairing activity of pulpal tissues.

Ideally, most of the required calcium phosphate should be released early as occurs with the above new formulations. If the material is adjacent to demineralized tooth structure, however, then additional sustained slow release from one interface to the other could help in remineralising teeth damaged by caries, improve mixing of the two interfaces and continue repair of the resin bond over a prolonged period. The latter could help combat bond strength decline that occurs with thermal and mechanical cycling and incomplete infiltration of the hybrid layer. The additional entrapment of CHX in this interfacial layer should furthermore prevent bacterial microleakage long term.

4.6. Antibacterial studies

The agar diffusion assay has been widely accepted as a simple screening method to assess the antibacterial properties of restorative materials [4]. However, this assay does not reflect the actual status in an oral cavity where the bacteria exist as

a biofilm which exhibit an increased resistance to antibacterial agents. In our study, we also measured the efficacy of the new formulations to inhibit bacterial biofilm growth using a CDFF model.

In the present study, two principle aetiological species of dental caries were selected for the agar diffusion assay, *Streptococcus mutans* and *Lactobacillus casei* [60,61]. Both of these have been specifically isolated from bacterial biofilms adherent to composite restorations [62]. In addition, *Actinomyces naeslundii* was also selected for study due to it is potential role in root surface caries [63].

Only CHX releasing formulations gave any significant antibacterial zone. These increased in size with raised PLR as expected since the average concentration of CHX released by formulations with high and low PLR at 48 hr was estimated as 56 and 39 μg/ml respectively. This confirmed that CHX was released from test materials in effective concentration to inhibit the growth of the organisms tested.

The agar diffusion assay results also confirmed that the antibacterial activity of test samples was purely due to CHX release. In our study, the lack of inhibition zones of Fuji II LC could be due to insufficient fluoride release. This finding has previously been reported for glass ionomer cements using the same test and similar bacterial species [64]. The greater effect of raising PLR on inhibition zones of *Actinomyces naeslundii*, could be attributed to the slower growth rate of this species.

In the more complex biofilm model system formulations with 5 % CHX in the monomer phase exhibited effective reduction in viable bacterial numbers on their surfaces. The effectiveness was also dependent upon PLR and hence on concentration of CHX released. The CHX-releasing experimental adhesives were more effective against the build-up of biofilm growth than commercially available fluoride releasing material, an effect that has been previously reported [7]. However, although the viable counts remained low throughout the experimental period compared to controls there was an increase in biofilm mass over time. This may be due to a reaction between the chlorhexidine and the artificial saliva. Indeed, the exchange of acetate with chloride salts of artificial saliva leads to the formation of insoluble salts and reduces CHX release from methacrylate polymers [65]. Furthermore, the effectiveness of antibacterial-releasing materials has also shown to

be reduced by the formation of a dead layer of bacterial cells on the surface, which may inhibit further killing, by reducing the penetration of antimicrobial agents [66].

4.7. Biological assessment

In this study, *in vitro* cell attachment to the new formulations has been evaluated using MG63 cells, a widely accepted cell line to evaluate osteoblast-like behaviour on various biomaterials [67]. The osteoblast cell line has been previously used to study the cytotoxicity of methacrylate based, calcium phosphate composites. [68]. The role of osteoblasts in initial stages of dentin reparation has also been reported [69].

The morphological characteristics and spreading behaviour of cells seeded for 24 h on material surfaces indicate early biocompatibility of the new formulations. This could be of clinical significance, as the material may then be applied into deep cavities or directly on pulpal tissues without potentially causing any cytotoxic effects and perhaps could play a role in reparative pulpal changes.

After immersion in growth medium, the crystals formed on tested formulations have Ca:P ratio 1.0 and 1.67 which correspond to that of brushite [$CaHPO_4.2H_2O$] and hydroxyapatite [$Ca_{10}(PO_4)_6.OH_2$], respectively. This may suggest that the Ca and PO_4 ions that have been released, reprecipitate on the material surface, forming crystals of different type, shape and size. The osteoconductive properties of hydroxyapatite and brushite are known to encourage cellular attachment and spreading [70, 71].

The chemical composition of the monomer phase [72] and degree of conversion [73] are considered the most important factors affecting the biocompatibility of polymer based dental materials. In this study, the addition of reactive calcium phosphate fillers to copolymer had no effect on the degree of conversion and the cellular attachment was evident on both composites and copolymer.

Although the material exhibited suitable properties as a liner/base material, further work may be needed to be undertaken to further improve the mechanical properties and to assess the bond strength of the new formulations to the tooth

structure. In addition, further studies are required using host cells such as odontoblasts and evaluation by more quantitative methods the effect of altering PLR and adding chlorhexidine on material biocompatibility.

5. Conclusion

Novel CHX-releasing calcium phosphate filled methacrylate based dental materials have been developed that could be used as an adhesive/liner with both antibacterial and remineralising activities. These new formulations have high degree of monomer conversion suitable for these clinical applications. Through the addition of MCPM, water sorption by the polymerised materials is encouraged, providing a means for CHX release. Through further addition of β–TCP, brushite formation within the polymer is encouraged providing a novel means to control water sorption and ion release. Any MCPM in molar excess of the β–TCP is released within 24 hours after placement of the polymerised formulations in water, which could be advantageous for dentine remineralization. In the presence of components of biological fluids, this calcium phosphate was observed to re - precipitate as a mixture of brushite and hydroxyapatite on the material surfaces. The calcium phosphate release level required for remineraliazation processes would depend upon the thickness of demineralised dentine layers but could be increased via raising the amount of excess MCPM e.g. by increasing the PLR. With higher PLR, CHX release increased as did inhibition of bacteria on both agar plates and in biofilms. Using an in vitro model for assessment of cell compatibility, the material was proven to be non toxic.

Acknowledgment

This project has been funded by the ministry of higher education- Libya. The authors would also like to thank Mrs Nicola J. Mordan for technical assistance with SEM.

References

[1] Brunthaler A, Koing F, Lucas T, Sperr W, Schedle A. Longevity of direct resin composite restorations in posterior teeth. Clin Oral Investig 2003;7:63-70.

[2] Splieth C, Rosin M, Gellissen B. Determination of residual dentine caries after conventional mechanical and chemomechanical caries removal with cariosolv. Clin Oral Investig 2001;5: 250-53.

[3] Beyth N, Domb AJ, Weiss EI. An in vitro quantitative antibacterial analysis of amalgam and composite resins. J Dent 2007;35:201-06

[4] Imazato S. Antibacterial properties of resin composites and dentin bonding systems. Dent Mater 2003;19:449-57.

[5] Xu X, Burgess JO. Compressive strength, fluoride release and recharge of fluoride releasing materials. Biomaterials 2003;24:2451-61.

[6] Kramer N, Garcia-Godoy F, Frankenberger R. Evaluation of resin composite materials. Part II: In vivo investigations. Am J Dent 2005;18:75-81.

[7] Leung D, Spratt DA, Pratten J, Gulabivala K, Mordan NJ, Young AM. Chlorhexidine-releasing methacrylate dental composite materials. Biomaterials 2005;26:7145-53.

[8] Dietrich TH, Losche AC, Losche GM, Roulet JF. Marginal adaptation of direct composite and sandwich restorations in CL II cavities with cervical margins in dentin. J Dent 1999:27:119-28.

[9] Hara AT, Queiroz CS, Freitas PM, Giannini M, Serra MC, Cury JA. Fluoride release and secondary caries inhibition by adhesive systems on root dentine. Eur J Oral Sci 2005;113:245-50.

[10] Wiegand A, Buchalla W, Attin T. Review on fluoride-releasing restorative materials—Fluoride release and uptake characteristics, antibacterial activity and influence on caries formation. Dent Mater 2007; 23:343-62.

[11] Estrela C, Sydney GD, Bammann LL, Felippe Junior O. Mechanism of action of calcium and hydroxyl ions of calcium hydroxide on tissue and bacteria. Braz Dent J 1995; 6:85-90

[12] Mongkolnam P, Tyas MJ. Light-cured lining materials: a laboratory study. Dent Mater 1994;10:196-202.

[13] Fernandes AM, Silva GA, Lopes NJr, Napimoga MH, Benatti BB, Alves JB. Direct capping of human pulps with a dentin bonding system and calcium hydroxide: an immunohistochemical analysis. Oral Surg Oral Med Oral Pathol Oral Radiol Endod 2008;105:385-90.

[14] Imazato S, Imai T, Ebisu S. Antibacterial activity of proprietary self-etching primers. Am J Dent 1998;11:106-8.

[15] Schmalz G, Ergucu Z, Hiller KA. Effect of dentin on the antibacterial activity of dentin bonding agents. J Endod 2004;30:352-58.

[16] Gondim JO, Duque C, Hebling J, Giro EM. Influence of human dentine on the antibacterial activity of self-etching adhesive systems against cariogenic bacteria. J Dent 2008;36:241-48.

[17] Meiers JC, Miller GA. Antibacterial activity of dentin bonding systems, resin-modified glass ionomers, and polyacid-modified composite resins. Oper Dent 1996;21:257-64.

[18] Schweikl H, Schmalz G. Glutaraldehyde-containing bonding agents are mutagens in mammalian cells in vitro. J Biomed Mater Res 1997;36:284-88.

[19] Imazato S, Kuramoto A, Takahashi Y, Ebisu S, Peters MC. In vitro antibacterial effects of the dentin primer of clearfil protect bond. Dent Mater 2006;22:527-32.

[20] Feuerstein O, Matalon S, Slutzky H, Weiss EI. Antibacterial properties of self-etching dental adhesive systems. J Am Dent Assoc 2007;138:349-54.

[21] Young AM, Chapter 27. Direct aesthetic tooth restoration materials. in Drug device combination products. A.Lewis Ed. Woodhead, Submitted Jan 2009.

[22] Xu HHK, Sun L, Weir MD, Antonucci JM, Takagi S, Chow LC, Peltz M. Nano DCPA-whisker composites with high strength and Ca and PO_4 release. J Dent Res 2006;85:722-27.

[23] Hofmann MP, Young AM, Gbureck U, Nazhat SN, Barralet JE (2006). FTIR-monitoring of a fast setting brushite bone cement: effect of intermediate phases. Journal of Materials Chemistry 2006;16:3199-3206.

[24] Costa CA, Mesas AN, Hebling J. Pulp response to direct capping with an adhesive system. Am J Dent 2000;13:81-87.

[25] Yuan H, Li Y, de Bruijn JD, Groot K, Zhang X. Tissue responses of calcium phosphate cement: a study in dogs. Biomaterials 2000;21:1283-90

[26] Goldberg M. In vitro and in vivo studies on the toxicity of dental resin components: a review. Clin Oral Investig 2008;12:1-8

[27] Anusavice KJ, Zhang NZ, Shen C. Controlled release of chlorhexidine from UDMA-TEGDMA resin. J Dental Res 2006;85:950-54.

[28] Sideridou I, Tserki V, Papanastasiou G. Effect of chemical structure on degree of conversion in light-cured dimethacrylate-based dental resins. Biomaterials 2002;23:1819-29.

[29] Young AM, Man Ho S, Abou Neel, EA, Ahmed I, Barralet, JE, Knowles, JC, Nazhat, SN. Chemical characterization of a degradable polymeric bone adhesive containing hydrolysable fillers and interpretation of anomalous mechanical properties. Acta Biomaterialia 2009 in press doi:10.1016/j.actbio.2009.02.022.

[30] Young AM, Ng PYJ, Gbureck U, Nazhat SN, Barralet JE, Hofmann MP. Characterization of chlorhexidine-releasing, fast-setting, brushite bone cements. Acta Biomaterialia 2008;4:1081-1088.

[31] Palin WM, Fleming GJ, Marquis PM. The reliability of standardized flexure strength testing procedures for a light-activated resin-based composite. Dent Mater 2005;21:911-19.

[32] Hengtrakool C, Pearson GJ, Wilson M. Interaction between GIC and S.sanguis biofilms: Antibacterial properties and changes of surface hardness. J Dent 2006;34:588-97.

[33] Pratten J, Wills K, Barnett P, Wilson M. In vitro studies of the effect of antiseptic-containing mouth washes on the formation and viability of streptococcus sanguis biofilms. J Appl Microbiol 1998;84:1149-55.

[34] Santos C, Clarke RL, Braden M, Guitian F, Davy KWM. Water absorption characteristics of dental composites incorporating hydroxyapatite filler. Biomaterials 2002:23:1897-1904.

[35] Mukerjee R, CFJ Wu. A modern theory of factorial design (Springer series in statistics), Springer-Verlag New York (2006).

[36] Young AM and Ho SM. Drug release from injectable biodegradable polymeric adhesives for bone repair. J Control Release 2008:127:162-72.

[37] Malacarne J, Carvalho RM, de Goes MF, Svizero N, Pashley DH, Tay FR, Yiu CK, de Oliviera Carrilho MR.. Water sorption/solubility of dental adhesive resins. Dent Mater 2006;22:973-80.

[38] Skrtic D, Antonucci JM. Dental composites based on amorphous calcium phosphate—Resin composition/physicochemical properties study. J Biomater Appl 2007;21:375-93.

[39] Braga RR, Ferracane JL. Contraction stress related to degree of conversion and reaction kinetics. J Dent Res 2002;81:114-18.

[40] Young AM, Rafeeka SA, Howlett JA. FTIR investigation of monomer polymerisation and polyacid neutralisation kinetics and mechanisms in various aesthetic dental restorative materials. Biomaterials 2004;25:823-33.

[41] Xia WZ and Cook WD. Exotherm control in the thermal polymerization of nona-ethylene glycol dimethacrylate (NEGDM) using a dual radical initiator system. Polymer 2003;44:79-88.

[42] Abou Neel EA, Young AM, Nazhat SN, Knowles JC. A Facile Synthesis Route to Prepare Microtubes from Phosphate Glass Fibres. Advanced Materials 2007;19:2856-62.

[43] Arima T, Hamada T, McCabe JF. The effects of cross-linking agents on some properties of HEMA based resins. J Dental Res 1995;74:1597-1601.

[44] Jedrychowski JR, Caputo AA, Kerper S. Antibacterial and mechanical properties of restorative materials combined with chlorhexidines. J Oral Rehabil 1983;10:373-81.

[45] Park MS, Eanes ED, Antonucci JM, Skrtic D. Mechanical properties of bioactive amorphous calcium phosphate/methacrylate composites. Dent Mater 1998;14:137-41.

[46] Lee SY, Regnault WF, Antonucci JM, Skrtic D. Effect of particle size of an amorphous calcium phosphate filler on mechanical strength and ion release of polymeric composites. J Biomed Mater Res 2007;80:11-17.

[47] Antonucci JM and Skrtic D. Matrix resin effects on selected physicochemical properties of amorphous calcium phosphate composites. J Bioact compat polym 2005;20:29-49.

[48] Lewis BA, Burgess JO, Gray SE. Mechanical properties of dental base materials. Am J Dent 1992;5:69-72.

[49] Craig RG. Restorative dental materials, Mosby, vol 10, St.Louis. 1997:173-208

[50] Skrtic D, Antonucci JM, Eanes ED. Amorphous calcium phosphate-based bioactive polymeric composites for mineralized tissue regeneration. J Res Nat Inst Stand Technol 2003;108:167-82.

[51] Skrtic D, Antonucci JM. Effect of bifunctional co-monomers on mechanical strength and water sorption of amorphous calcium phosphate- and silanized glass-filled Bis-GMA-based composites. Biomaterials 2003;24:2881-88.

[52] Patel MP, Cruchley AT, Coleman DC, Swai H, Braden M, Williams DM. A polymeric system for the intra-oral delivery of an anti-fungal agent. Biomaterials 2001;22:2319-24.

[53] Carrilho MRO, Carvalho RM, De Goes MF, Di HipolitoV, Geraldelis FR, Tay FR, Pashley DH, Tjaderhane L. Chlorhexidine preserves dentin bond in vitro. J Dent Res 2007:86:90-94.

[54] Elliot JC. General chemistry of the calcium orthophosphate. Structure and Chemistry of apatites and other calcium orthophosphates. Studies in Inorganic chemistry, vol.18, Elsevier, Amsterdam 1994:1-6.

[55] Dickens SH, Flaim GM, Takagi S. Mechanical properties and biochemical activity of remineralizing resin-based Ca-PO_4 cements. Dent Mater 2003;19:558-66.

[56] Tziafas D, Alvanou A, Kaidoglou K. Dentinogenic activity of allogenic plasma fibronectin on dog dental pulp. J Dent Res 1992;71:1189-95.

[57] Murray PE, About I, Franquin JC, Remusat M, Smith AJ. Restorative pulpal and repair responses. J Am Dent Assoc 2001;132:482-91.

[58] Murrary PE, Hafez AA, Smith AJ, Cox CF. Bacterial microleakage and pulpal inflammation associated with various restorative materials. Dent Mater 2002;18:470-478.

[59] Mizuno M, Banzai Y. Calcium ion release from calcium hydroxide stimulated fibronectin gene expression in dental pulp cells and the differentiation of dental pulp cells to mineralized tissue forming cells by fibronectin. Int Endod J 2008;41:933-38.

[60] Bjørndal L, Larsen T. Changes in cultivable flora in deep carious lesions following a stepwise excavation procedure. Caries Res 2000;34:502-508

[61] Martin FE, Nadkarni MA, Jacques NA, Hunter N. Quantitative microbiological study of human carious dentine by culture and real time PCR: association of anaerobes with histopathological changes in chronic pulpitis. J Clinic Microbiol 2002;40:1698-1704.

[62] Kidd EAM, Beighton D. Prediction of secondary caries around tooth-colored restorations: A clinical and microbiological study. J Denta Res 1996;75:1942-46.

[63] Bowden GH, Nolette N, Ryding H, Cleghorn BM. The diversity and distribution of predominant ribotypes of actinomyces naeslundii genospecies 1 and 2 in samples from enamel and from healthy and carious root surfaces of teeth. J Dent Res 1999;78:1800-1809.

[64] Takahashi Y, Imazato S, Kaneshiro AV, Ebisu S, Frencken JE, Tay FR. Antibacterial effects and physical properties of glass ionomer cements containing chlorhexidine for the ART approach. Dent Mater 2006;22:647-52.

[65] Nerurkar MJ, Zentner GM, Rytting JH. Effect of chloride on the release of CHX salts from methyl methacrylate: 2-hydroxyethyl methacrylate copolymer reservoir devices. J Control Release 1995;33:357-63.

[66] Valappil SP, Pickup DM, Carroll DL, Hope CK, Pratten J, Newport RJ, Smith ME, Wilson M, Knowles JC. Effect of silver content on the structure and antibacterial activity of silver-doped phosphate-based glasses. Antimic Agents Chemother 2007;51:4453-61.

[67] Abou Neel EA, Knowles JC. Physical and biocompatibility studies of novel titanium dioxide doped phosphate-based glasses for bone tissue engineering applications. J Mater Sci Mater Med 2008:19:377-86.

[68] Simon CG, Antonucci JM, Liu DW, Skrtic D. In vitro cytotoxicity of amorphous calcium phosphate composites. J Bioact Compat Polym 2005;20:279-95.

[69] Goldberg M, Lacerda-Pinheiro S, Jegat N, Six N, Septier D, Priam F, Bonnefoix M, Tompkins K, Chardin H, Denbesten P, Veis A, Poliard A, Gunduz M. Bioactive

molecules stimulate tooth repair and regeneration. J Hard Tissue Biology 2006;15:36-45.

[70] Moursi AM, Winnard AV, Winnard PL, Lannutti JJ, Seghi RR. Enhanced osteoblast response to a polymethylmethacrylate-hydroxyapatite composite. Biomaterials 2002;23:133-44.

[71] Feng C, Blanchemain N, Lefevre A, Hildebrand HF. In vitro studies on influence of precultural conditioning method on osteoblast reactions of a new type of injectable calcium cement material. J Biomed Mater Res. 2006;77:104-13.

[72] Al-Hiyasat AS, Darmani H, Milhem MM. Cytotoxicity evaluation of dental resin composites and their flowable derivatives. Clin Oral Investig 2005:9:21-25.

[73] Tseng WY, Huang CH, Chen RS, Lee MS, Chen YJ, Rueggeberg FA, Chen MH. Monomer conversion and cytotoxicity of dental composites irradiated with different modes of photoactivated curing. J Biomed Mater Res 2007:83:85-90.

List of Figures

Fig. 1. Representative average Raman spectra of an experimental adhesive with high PLR, small MCPM particle diameter and 5wt % CHX, before and at 24 hr post-curing followed by an additional 24 hours immersion in deionised water. Spectra exhibit monomer peaks at 1400 / 1638, β – TCP at 943 / 968, MCPM at 901/912/1011, brushite at 986 and CHX at 1288/1294 $cm.^{-1}$

Fig. 2. $2a_i$ values (see equations 11-14) for degree of conversion and dry and wet compressive and biaxial flexural strengths of experimental adhesives with variables PLR, MCPM particle diameter and CHX concentration. Error bars are 95 % C.I. The symbol (*) refers to $2a_i$ values that are significantly different from zero. Interaction terms were negligible so not shown.

Fig. 3. Mass changes in deionised water or phosphate buffer solution as a function of square root (SQRT) of time for experimental adhesives containing MCPM particles of 29 or 90 micron diameter. Filled and unfilled symbols refer to PLR of 3:1 and 1:1 respectively. As expected from equation 10 this plot is initially linear but reaches a maximum after 24 hours. Standard deviation of the reported values ranged from 0.3 to 1.2 wt % (n = 3).

Fig. 4. $2a_i$ values (see equations 11-14) for initial gradient and total cumulative CHX release, initial gradient of mass increase, maximum mass and volume increase, with variables PLR, MCPM particle diameter and type of storage solution. Error bars are 95 % C.I. The symbol (*) refers to $2a_i$ values that are significantly different from zero. Interaction terms were negligible and so not shown.

Fig. 5. CHX release into deionised water or phosphate buffer solution as a function of the square root of time (see equation 10) for experimental adhesives containing MCPM particles of 29 or 90 micron diameter. Filled and unfilled symbols refer to PLR 3:1 and 1:1 respectively. Standard deviation of the reported values ranged from 0.2 to 1.5 wt% (n = 3).

Fig. 6. Calcium and phosphate ion release kinetics of experimental adhesives prepared with high (filled symbols) and low (unfilled symbols) PLR and small MCPM particle diameter. The standard deviations of the reported values ranged from 0.05 to 0.1 mM and from 0.07 to 0.14 mM for calcium and phosphate respectively (n =3).

Fig. 7. Maximum concentrations of calcium and phosphate ions released from adhesive formulations with high or low PLR (with small or large MCPM particle diameter) after 2 weeks of immersion in deionised water. The symbol (*) refers to formulations which have significantly different results when compared with the sample with PLR 1:1 and MCPM p.d 29 μm. Error bars represent 95 % C.I of the mean (n = 3).

Fig. 8. Inhibition zones observed in agar diffusion tests for adhesive formulations prepared with variable PLR and MCPM particle diameter. The symbol (*) refers to formulations which have

significantly different results when compared with the sample with PLR 1:1 and MCPM p.d 29 µm. The error bars refer to 95 % C.I of the mean (n=3).

Fig. 9. The number of CFU on RMGIC (Fuji II LC), and experimental adhesives after 6, 24 and 72hr in a CDFF. Error bars refer to 95 % C.I (n=3). The symbol (*) refers to formulations which have significantly different results at a given time when compared with both formulation (I) and Fuji II LC. Formulation (I) contains 0 % CHX, PLR 3:1. Formulation (II) and (III) contains 5 % CHX with PLR 1:1 or 3:1 respectively.

Figure 10. SEM micrographs of cells on different surfaces: (a) Thermanox ® (b) unfilled copolymer (c) formulation with PLR 1:1 (d) formulation with PLR 3:1.

List of Tables:

Table 1. (a) and (b) Physico-chemical properties of different adhesive formulations containing reactive calcium phosphate fillers and UDMA/TEGDMA/HEMA based resin. The initial mass and chlorhexidine gradients were calculated using data up to 6 hr and 1 week respectively, whereas the maximum mass and volume increase was obtained at 24hr. Geometric mean refers to that of all 8 formulations. The errors represents the standard deviation of the mean (n=8 and 3 in a and b respectively).

Figure 1

Fig.1

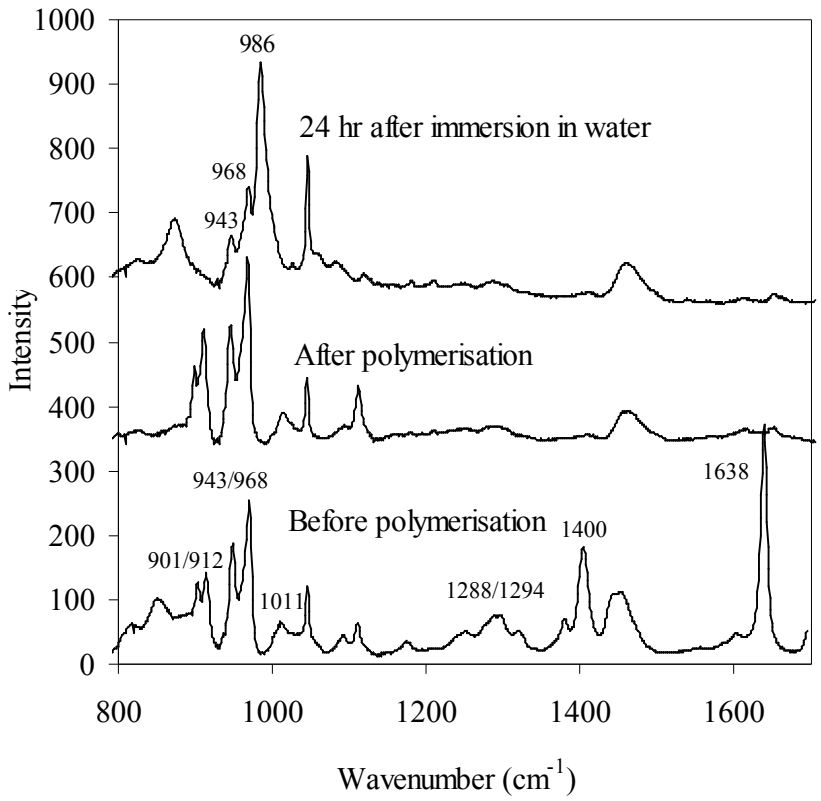

Fig. 2

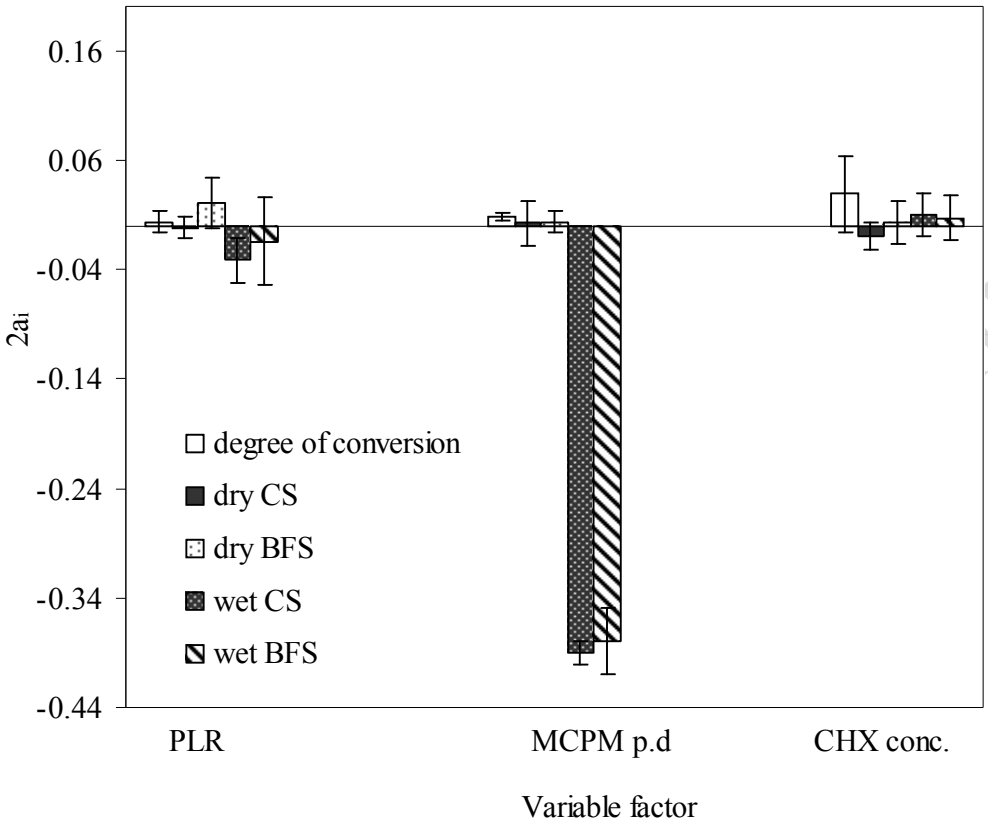

Fig. 3

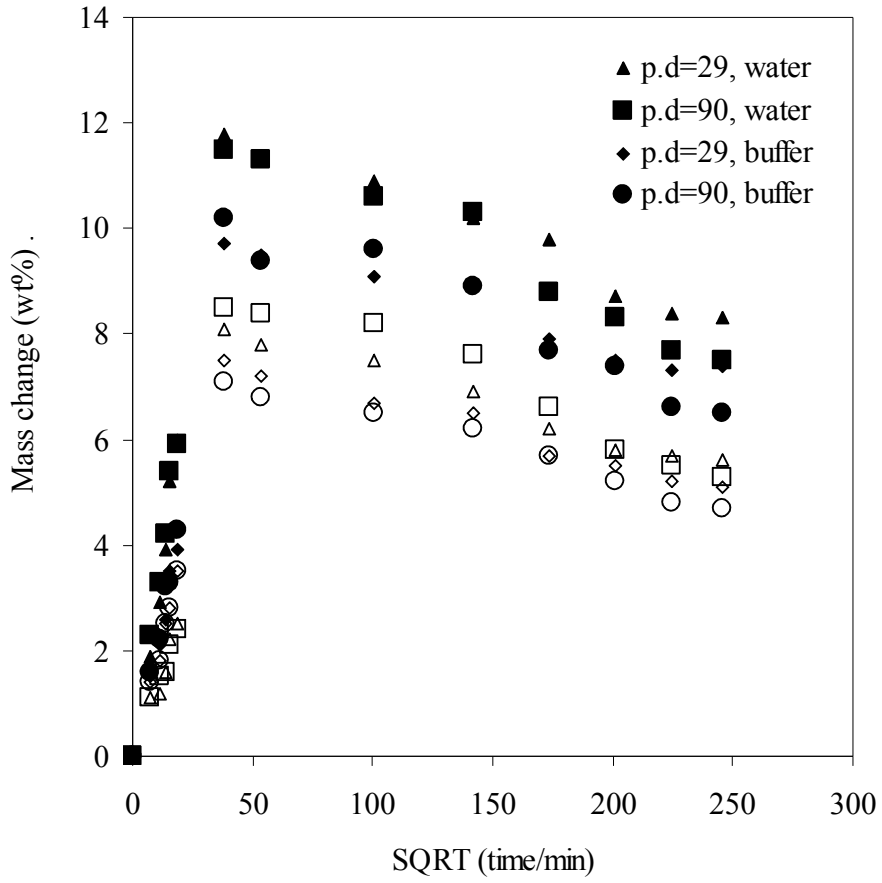

Fig. 4

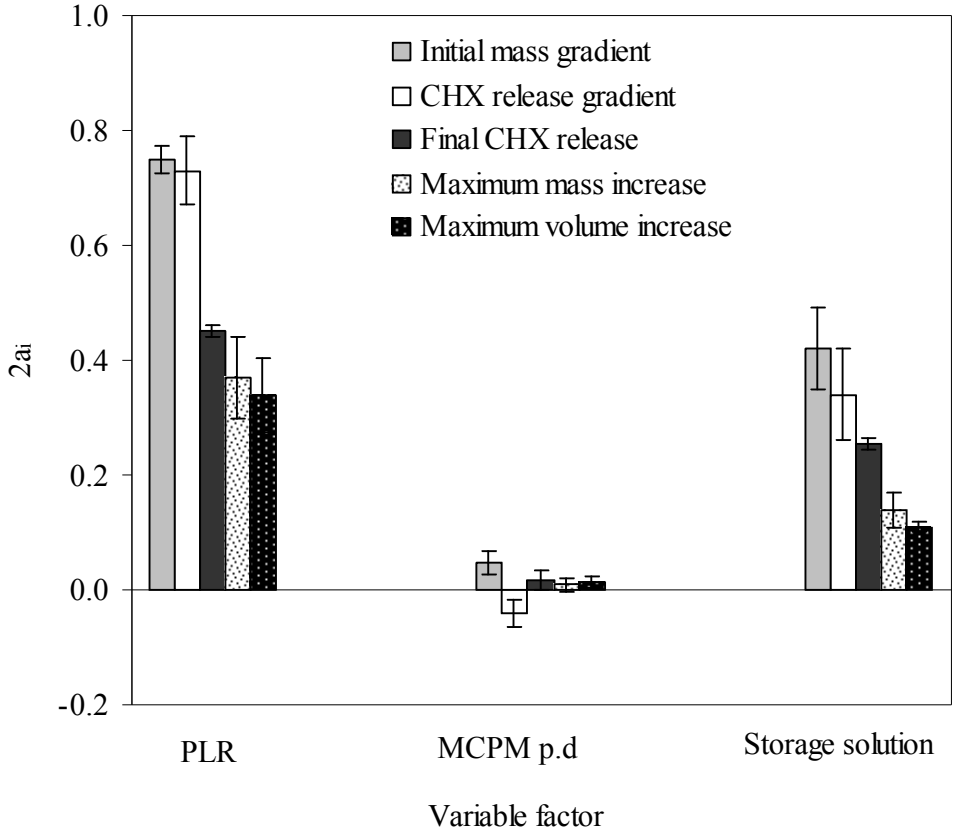

Fig. 5

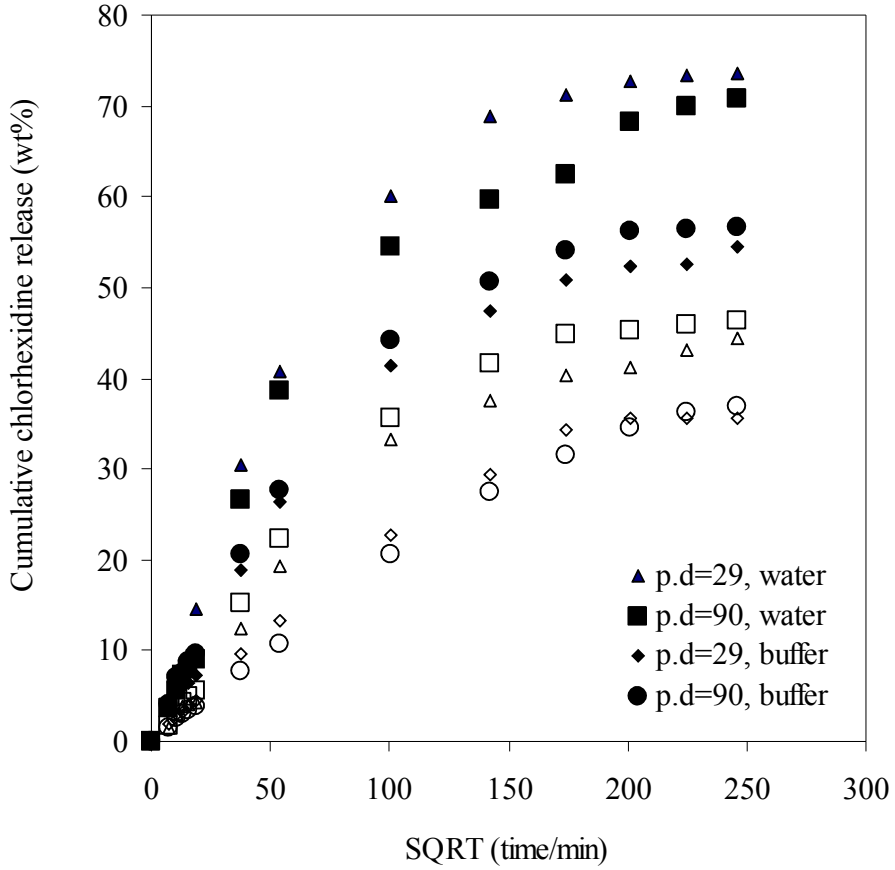

Fig. 6

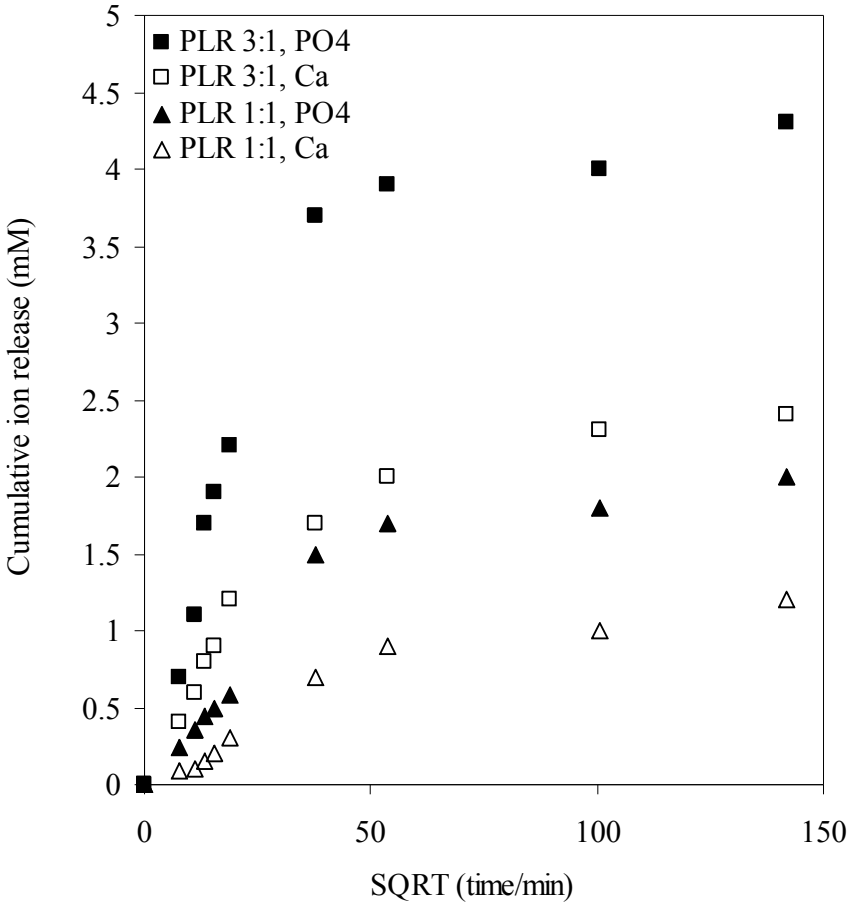

Fig. 7

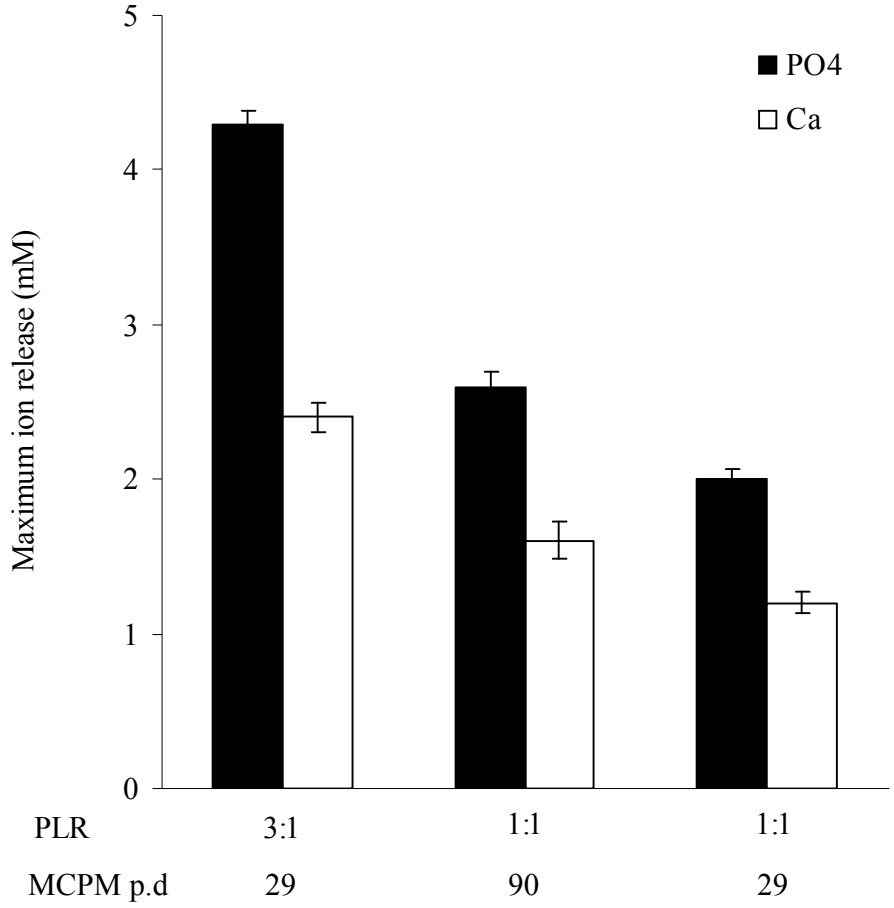

Fig. 8

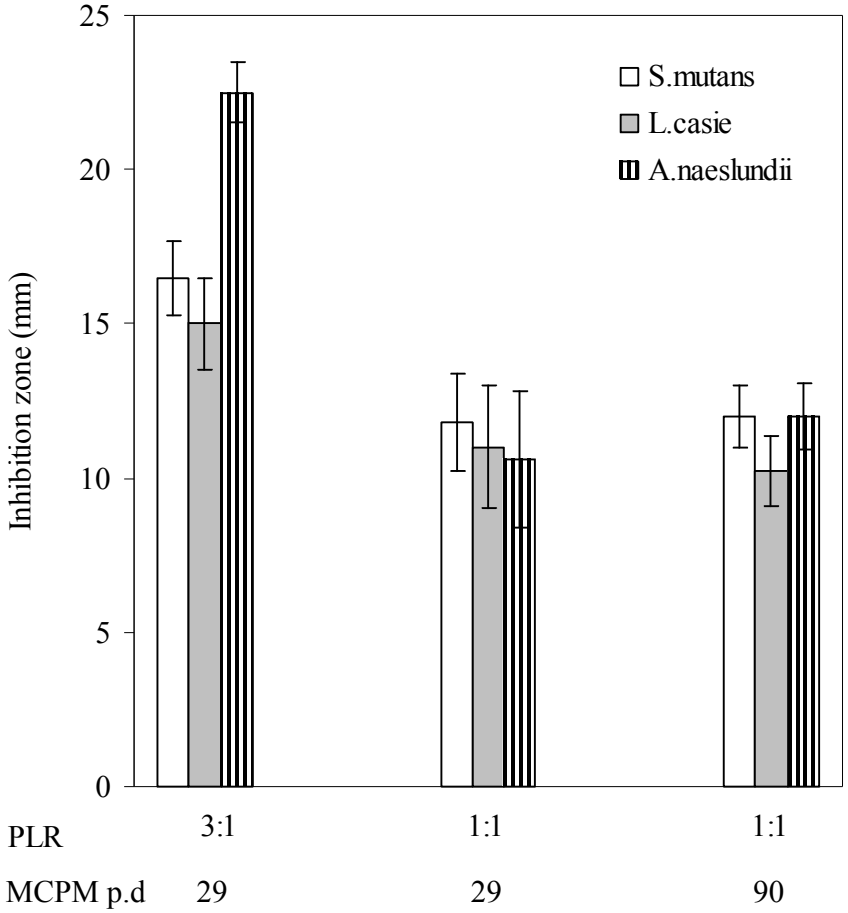

Fig. 9

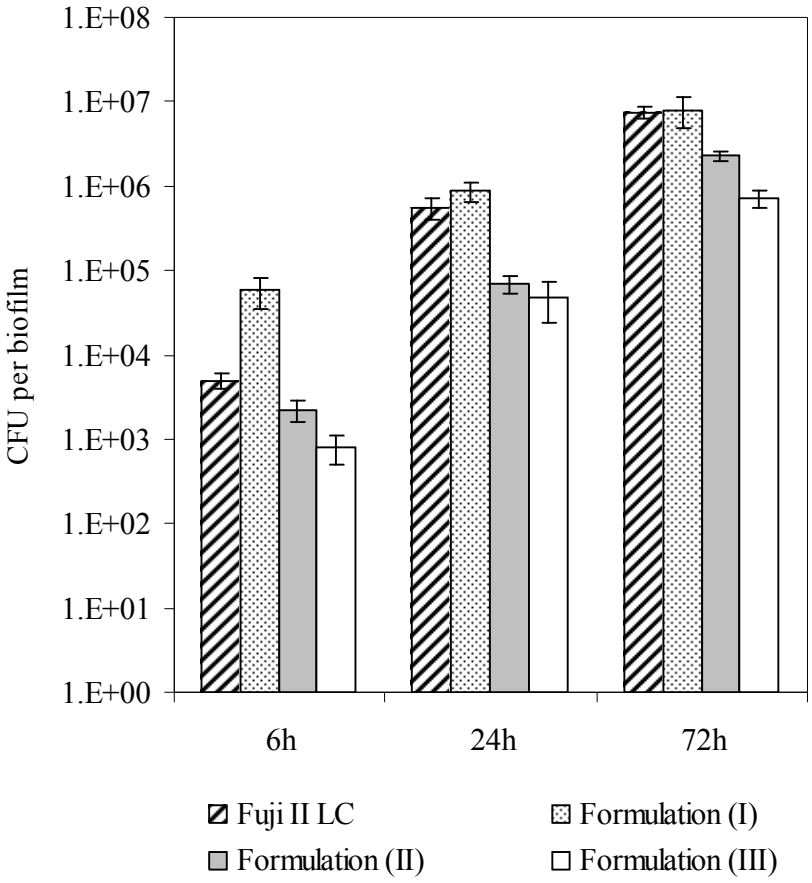

Fig. 10

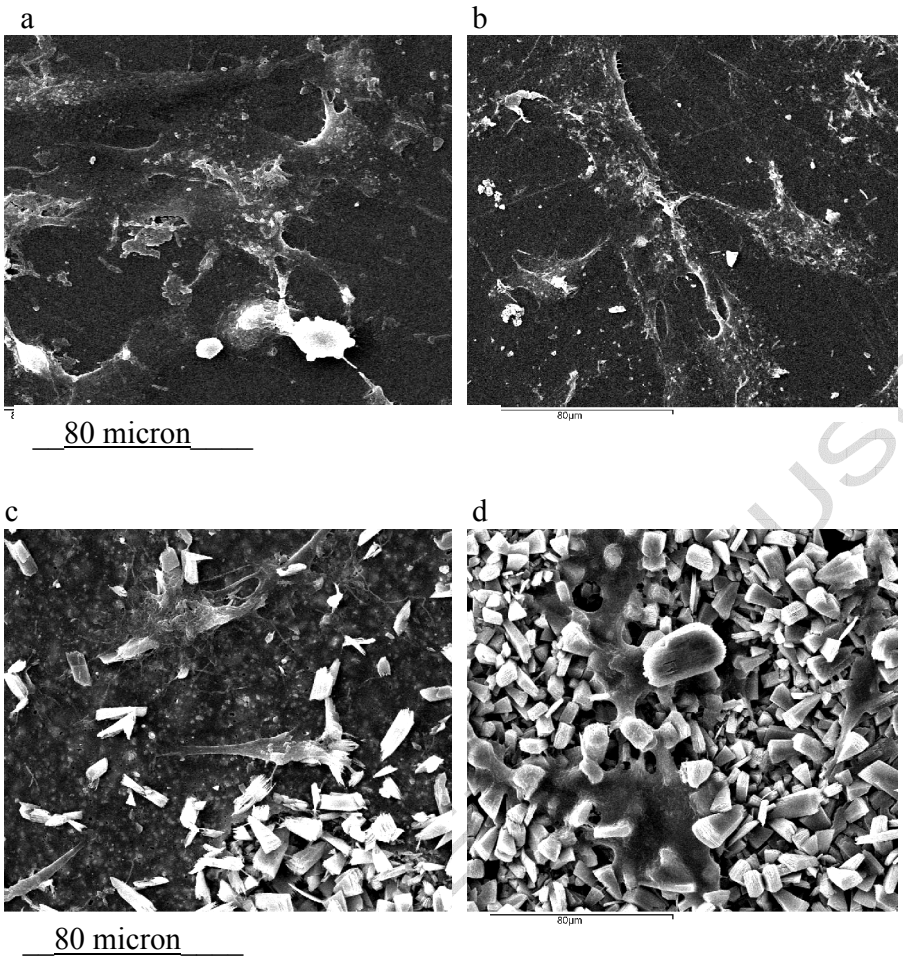

Table 1:
(a)

PLR	MCPM (μm)	P.S. (wt %)	CHX	Degree of conversion (%)	Compressive strength (MPa)			Biaxial flexure strength (MPa)		
					Dry	24hr	1week	Dry	24hr	1week
3:1	29	5		91 ± 3	85 ± 4	39 ± 3	41 ± 3	61 ± 2	33 ± 2	34 ± 2
3:1	29	0		87 ± 1	87 ± 2	38 ± 3	40 ± 3	60 ± 3	32 ± 3	33 ± 2
3:1	90	5		92 ± 2	88 ± 4	26 ± 3	27 ± 3	62 ± 3	22 ± 2	23 ± 2
3:1	90	0		88 ± 2	87 ± 3	25 ± 2	27 ± 2	62 ± 2	21 ± 2	22 ± 3
1:1	29	5		91 ± 2	87 ± 4	40 ± 4	42 ± 2	61 ± 3	32 ± 2	33 ± 2
1:1	29	0		88 ± 1	88 ± 2	37 ± 3	39 ± 4	60 ± 3	32 ± 3	32 ± 4
1:1	90	5		92 ± 3	86 ± 3	28 ± 2	29 ± 3	59 ± 3	22 ± 2	23 ± 2
1:1	90	0		88 ± 1	87 ± 3	25 ± 3	27 ± 3	60 ± 3	23 ± 2	24 ± 3
Geometric mean:				90	87	32	34	61	27	28
ln geometric mean (<LnP>):				4.5	4.5	3.5	3.5	4.0	3.3	3.3

(b)

PLR	MCPM p.d (μm)	Storage solution	Initial mass gradient (wt %/min$^{0.5}$)	Maximum mass increase (wt %)	Maximum volume increase (vol%)	CHX release gradient (wt %)	Final CHX release (wt %)	CHX diffusion coefficient (cm^2/s)
3:1	29	D.W	0.31 ± 0.01	11.8 ± 0.6	24.3 ± 0.7	0.65 ± 0.05	74 ± 1	0.27×10^{-8}
3:1	29	PBS	0.20 ± 0.02	9.7 ± 0.5	20.5 ± 0.4	0.43 ± 0.01	54 ± 2	0.12×10^{-8}
3:1	90	D.W	0.32 ± 0.02	11.5 ± 0.2	23.4 ± 0.7	0.58 ± 0.03	71 ± 1	0.22×10^{-8}
3:1	90	PBS	0.21 ± 0.02	10.2 ± 0.7	21.4 ± 0.3	0.47 ± 0.03	57 ± 2	0.14×10^{-8}
1:1	29	D.W	0.12 ± 0.02	8.0 ± 0.6	16.5 ± 1.0	0.30 ± 0.02	44± 1	0.058×10^{-8}
1:1	29	PBS	0.10 ± 0.02	7.5 ± 0.2	15.2 ± 1.2	0.23 ± 0.02	36 ± 1	0.034×10^{-8}
1:1	90	D.W	0.17 ± 0.01	8.5 ± 0.4	17.5 ± 0.5	0.35 ± 0.02	46 ± 1	0.079×10^{-8}
1:1	90	PBS	0.10 ± 0.01	7.0 ± 0.5	15.3 ± 1.1	0.20 ± 0.03	37 ± 2	0.026×10^{-8}
Geometric mean:			0.17	9.0	19	0.38	53	0.09×10^{-8}
ln geometric mean (<LnP>):			-1.8	2.2	2.9	-0.96	3.9	-2.4×10^{-8}